Investigation of the Possibility of Obtaining Nickel-Containing Ferroalloys from Lateritic Nickel Ores by a Metallothermic Method

Assylbek Abdirashit [1,*], Dauren Yessengaliyev [1,*], Bauyrzhan Kelamanov [1], Otegen Sariyev [1], Gulnur Abikenova [2], Nurzhan Nurgali [2], Maral Almagambetov [2], Talgat Zhuniskaliyev [3], Yerbol Kuatbay [4] and Zhanmurat Abylay [1]

[1] Department of Metallurgy and Mining, K. Zhubanov Aktobe Regional University, Aktobe 030000, Kazakhstan; bkelamanov@zhubanov.edu.kz (B.K.); osariyev@zhubanov.edu.kz (O.S.); zhabylay@zhubanov.edu.kz (Z.A.)

[2] ERG Research and Engineering Center, Astana 010000, Kazakhstan; gulnur.abikenova@erg.kz (G.A.); nurzhan.nurgali@erg.kz (N.N.); maral.almagambetov@erg.kz (M.A.)

[3] Department of Science, Eurasian Technological University, Almaty 050000, Kazakhstan; t.zhuniskaliyev@tttu.edu.kz

[4] Department of Metallurgy and Materials Science, Karaganda Industrial University, Temiratau 101400, Kazakhstan; ye.kuatbay@tttu.edu.kz

* Correspondence: a.abdirashit@tttu.edu.kz (A.A.); dyessengaliyev@zhubanov.edu.kz (D.Y.); Tel.: +7-707-460-10-20 (A.A.)

Abstract: This study presents the results of laboratory experiments on the processing of lateritic nickel ores mixed with coal and CaO, followed by the use of the obtained product for the smelting of nickel-containing ferroalloy by the metallothermic method. The study analyzed the thermodynamic effects of complex reductant concentration (silicon- and aluminum-containing alloy) on the reduction degree of nickel and iron. An experimental process resulted in a product containing Ni_{total} (2.60%) and Fe_{total} (60.52%), obtained through reduction roasting of lateritic nickel ore mixed with coal and an addition of 20 g of CaO at a temperature of 1150 °C. Under laboratory conditions, a nickel-containing ferroalloy was successfully obtained using the product after reduction roasting and a complex alloy as the reducing agent. The following optimal process parameters were determined: reductant consumption of 20 g per 100 g of the reduction roasting product, smelting temperature of 1600 °C, and slag basicity (CaO/SiO_2) of 0.5. In this case, a nickel-containing ferroalloy with 72% iron, 15% nickel, and up to 5% chromium was successfully obtained through silicon and aluminum reduction using a complex alloy. A microstructural analysis of the nickel-containing alloy was conducted using an electron probe microanalyzer (JXA-8230) in combination with scanning electron microscopy (SEM) and energy-dispersive X-ray spectroscopy (EDS). The results showed that silicon and iron were the dominant elements in all particles. Nickel was detected at concentrations of up to 15.02 wt. %, while chromium reached 3.47 wt. %. Depending on the silicon concentration, the nickel-containing ferroalloy is recommended for corrosion-resistant steel production (Si < 5%) and as a reducing agent for ferronickel production (Si > 5%).

Keywords: laterite nickel ore; nickel-containing ferroalloys; silicon- and aluminum-containing reductant; metallothermic method; thermodynamic modeling

1. Introduction

The development of nuclear energy, electronics, jet technology, and the mechanical engineering industry contributes to the further progress of various sectors, including the metallurgical industry.

Such technological advancements would be impossible without the use of alloys with special physicochemical properties, such as high strength, heat resistance, corrosion resistance, and chemical stability. The production of such alloys involves various metals, including nickel-containing ferroalloys. In market conditions, the rational and efficient utilization of mineral resources is of great importance, including improving the quality of metallurgical products and enhancing processing technologies. The same approach is required for the electrometallurgy of nickel ferroalloys. As for the Republic of Kazakhstan, the production of nickel-containing ferroalloys has not yet been established due to the absence of an appropriate technology for processing lateritic nickel ores. At the same time, Kazakhstan has sufficient reserves of lateritic nickel ores, and it is among the top 20 countries in terms of nickel reserves, with global reserves of 2% (1.5 million tons) [1–3]. Nickel ore consists of 30% sulfide nickel ore and 70% oxide nickel ore (mainly lateritic nickel ore). Nickel production from oxidized or lateritic ores is indeed gaining popularity, but currently, a significant portion of global production still comes from sulfide nickel ores. However, given the limited reserves of sulfide ores and the growing demand for nickel in metallurgical technologies, the use of lateritic ores is becoming increasingly important and relevant [4–10].

Lateritic nickel ores are typically found in tropical or subtropical regions, where ultrabasic rocks rich in iron and magnesium are formed as a result of weathering. These deposits typically consist of different layers due to weathering conditions, such as a silica-rich layer, a limonite layer dominated by goethite [$FeO(OH)$] and hematite [(Fe_2O_3)], and a saprolite layer [($Ni,Mg)SiO \cdot nH_2O$)], which is rich in magnesium and essential elements [11–13]. Regarding the processing technology of lateritic nickel ores, various technological schemes exist for their processing. The Rotary Kiln-Electric Furnace process is used for nickel production from lateritic ores, where the ores are first subjected to thermal treatment in a rotary kiln, where reduction and sulfidization take place. The resulting product is then processed in an electric furnace for further nickel production. The disadvantages of this process are as follows: 1. High energy consumption: Rotary kilns and electric furnaces require significant energy to maintain the necessary temperatures, making the process energy-intensive and expensive. 2. Low nickel recovery: Despite the use of modern technologies, the process may not ensure a high recovery of nickel from lateritic ores. 3. Atmospheric pollution: During processing, harmful emissions such as sulfur oxides and carbon dioxide may be released, requiring additional costs for gas cleaning and compliance with environmental standards. These disadvantages can be reduced by optimizing the process and improving technologies, but overall, the Rotary Kiln-Electric Furnace route is less preferred compared to other nickel processing methods [14–16]. The main risks in the processing of oxidized nickel ores with high iron content using pyrometallurgical methods, such as the rotary kiln and electric furnace process, are the formation of clinker in the rotary kiln, which complicates the processing and reduces the efficiency of the equipment. Additionally, the aggressive behavior of the slag in the electric furnace is a concern. The slag becomes viscous, which can lead to damage to the lining of the equipment.

Yildirim et al. [17] presented the results of processing low-grade lateritic nickel ore using the carbothermic method to produce nickel pig iron. The ore used was from the Anatolian region of Eastern Turkey, containing 0.9% Ni, 0.054% Co, and 2.3% Cr. The study examined the effects of the amount of reductant, process duration, and flux quantity on metal recovery efficiency and concentration. As a result, nickel-chromium-containing pig iron was obtained with the following composition (%): Fe—90–92%; Ni—3.79–5.29%; Cr—1.79–2.45%; Co—0.17–0.23%. However, to achieve high nickel and chromium recovery using the aforementioned technology, a precise technological calculation of the charge material ratio is required due to the variability in nickel, iron, and chromium content in

lateritic ore, as well as the temperature conditions necessary for smelting nickel-chromium-containing pig iron.

There is a technology for processing oxidized nickel ores to obtain ferronickel, which was used at the American plant "Riddle". The essence of the technology lies in treating molten oxidized nickel ore in an electric furnace with ferrosilicon [18]. The metallothermic reduction of nickel facilitates the production of high-grade ferronickel from low-grade oxidized nickel ores without hazardous slag foaming by eliminating carbonaceous materials from the charge.

However, despite its advantages, a significant drawback of the known process is the use of an expensive reducing agent, ferrosilicon (FeSi 45). The consumption of ferrosilicon depends on the iron and nickel content in the melt. The iron from ferrosilicon transfers into ferronickel, thereby limiting the extraction of iron from the raw material. As a result, there is a known limit to the nickel content in the final product, exceeding which reduces nickel recovery. On the other hand, the reduction of large amounts of iron and the production of lower-grade products require an excessively high consumption of ferrosilicon. It has been established that the best technical and economic performance of the ferronickel production process is achieved when using an alloy containing 45% silicon.

In the study by Zayakin et al. [19], the results of ferronickel smelting from low-grade oxidized nickel ores using aluminum slag from aluminum production waste as a reducing agent are presented. The aluminum and silicon content in the aluminum slag was 21% and 1.5%, respectively. The consumption of aluminum slag ranged from 5 wt. % to 30 wt. % of the nickel ore mass. The results of semi-industrial trials demonstrated the fundamental feasibility of producing ferronickel by the aluminothermic method with a nickel content ranging from 15% to 20%.

Thus, as evidenced by the conducted analysis, metallothermic reduction of oxides positively influences the reaction process, intensifying them.

The objective of this study is the reduction roasting of laterite ore using a carbon-containing reductant and CaO, followed by the production of a nickel-containing ferroalloy by the metallothermic method. The scientific novelty of the work lies in the production of a nickel-containing ferroalloy using silicon- and aluminum-containing alloys from low-grade nickel ores as reducing agents.

2. Materials and Methods

2.1. Materials

A comparison of Kazakhstan's laterite nickel ores with those processed abroad shows that foreign facilities typically process nickel ores containing at least 1.2% Ni, with an average nickel content ranging from 1.9% to 2.5% [20–22]. Kazakhstani ores are lower in nickel content, averaging between 0.85% and 1.1% Ni [23].

The nickel ore used in this study was sourced from the "Kempirsai" deposit, located in the western part of Kazakhstan (Aktobe region). Based on its technological properties, the presented lateritic nickel ore most likely belongs to the iron-siliceous type. The chemical composition of the lateritic nickel ore is shown in Table 1. The image and X-ray diffraction pattern results of the lateritic nickel ore are presented in Figure 1.

Table 1. Chemical composition of lateritic nickel ore, %.

NiO	Fe_{total}	Cr_2O_3	SiO_2	MgO	CaO	Al_2O_3	P	LOI
1.01	18.37	2.57	45.11	6.5	0.18	2.71	0.005	23.55

(**a**)   (**b**)

(**c**)
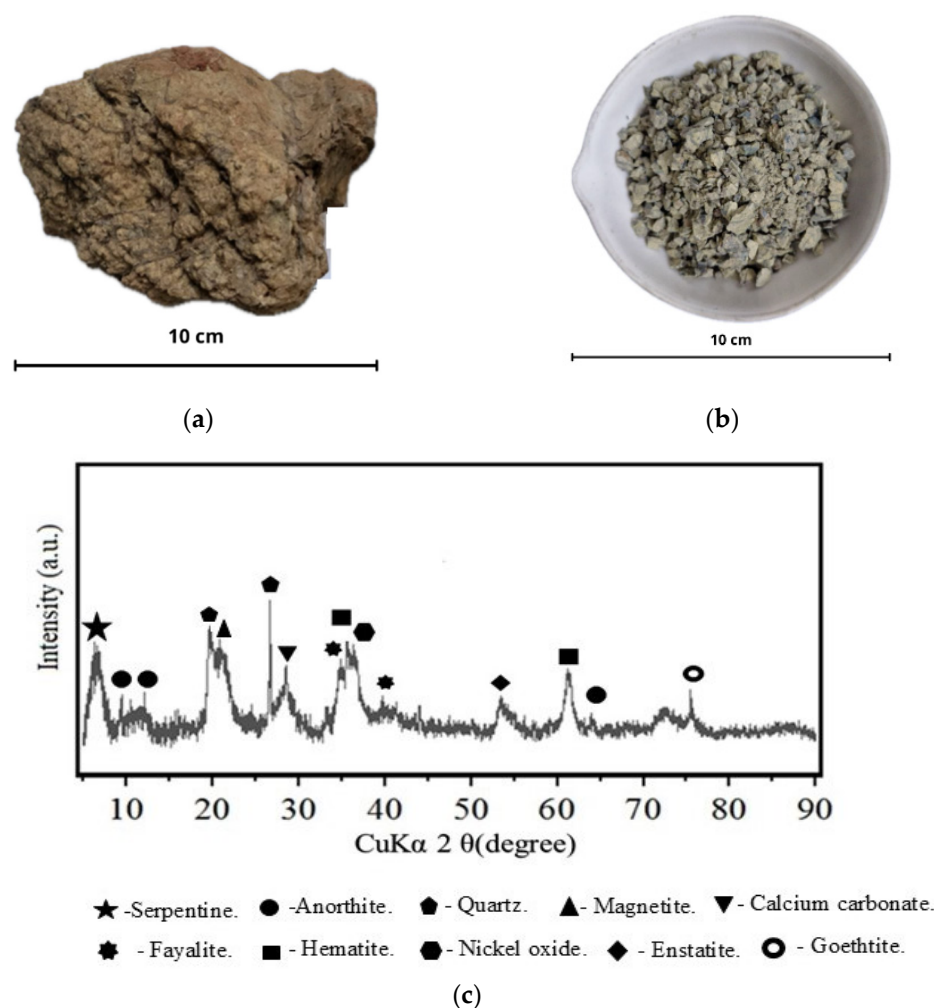
Figure 1. (**a**) Image of lumpy, (**b**) fine laterite ore (less than 4 mm), and (**c**) X-ray diffraction pattern result of laterite ore.

The studied lateritic nickel ore appears as a loose, hydrated, clay-like mass. Due to this, the raw nickel ore was dried at 200 °C for 6 h, resulting in a mass loss of approximately ~15.0%. After drying, a sample was taken from the ore and subjected to crushing using a hammer crusher (PC400x600, Runwell Co., Shanghai, China). After crushing, the ground ore was sieved through a wire mesh screen with a mesh size of −2 mm using a vibrating sieving machine (AS 200, Retsch, Verder, Germany) with a vibration amplitude of 1.5 and a sieving time of 60 s. The image of finely ground nickel ore is shown in Figure 1b. Further, samples of finely ground nickel ore were taken for X-ray phase analysis and thermal analysis. The phase composition of the lateritic nickel ore was determined using X-ray diffraction (XRD) analysis on a Rigaku Ultima IV X-ray diffractometer (XRD, Rigaku, The Woodlands, TX, USA), and the diffraction pattern was interpreted using the "Match! 3.0" software.

The obtained results show that the finely ground lateritic ore contains iron-bearing phases, including hematite, magnetite, and iron hydroxide, as well as varieties of quartz and fayalite. Complex phases such as anorthite and serpentine are also present. Nickel in this ore is primarily found as an isomorphic impurity in hydrated magnesium, aluminum, and iron silicates (serpentine). Additionally, nickel is also present as an adsorption product in silica and iron hydrogels.

To assess the kinetic characteristics occurring during the heating of lateritic nickel ores, differential thermal analysis (DTA) was performed using the STA 409 PC/PG Luxx

system (Evisa Co., Vienna, Austria) and the Q-1500D derivatograph (IOM companies, Budapest, Hungary). This method allows the study of physical and chemical transformations accompanied by thermal effects. The principle of DTA is based on measuring the temperature difference between the sample under investigation and a reference material during simultaneous heating. The temperature difference that arises during heating or cooling is caused by endothermic or exothermic reactions in the studied material. The DTA system records changes in mass (TG), mass change rate (DTG), and the temperature difference (DSC) between the sample and an inert reference material under continuous heating at a set rate of 10 °C per minute [24–26].

The results of the differential thermal analysis in an argon atmosphere are presented in Figure 2.
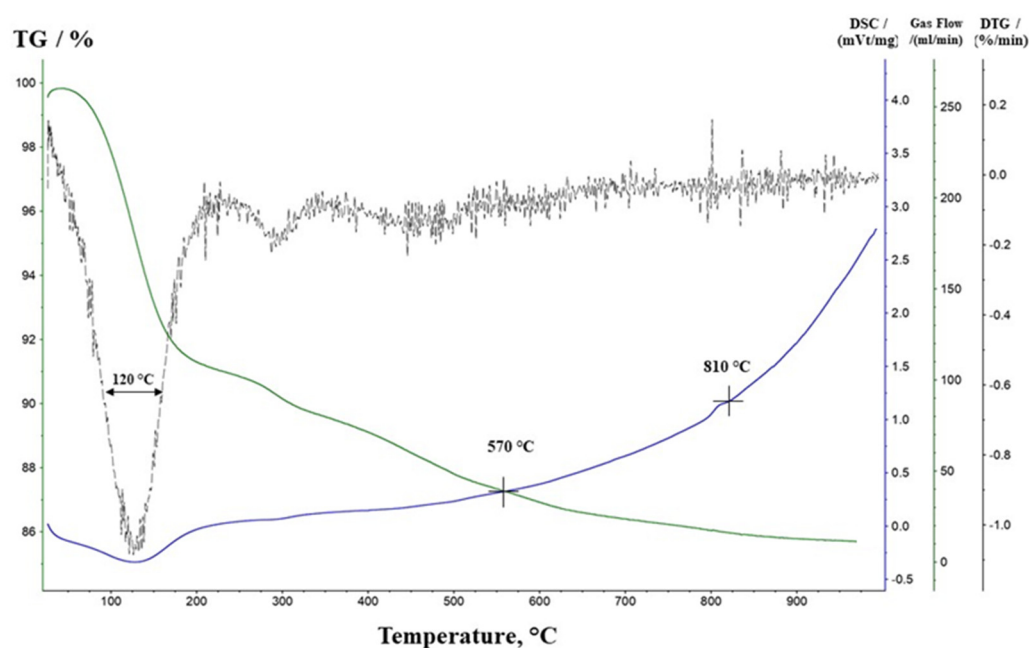

Figure 2. Thermogram of lateritic nickel ore heating in an argon atmosphere. Curve labels: TG—Change in sample mass (thermography), DSC—Curve of differential temperature, DTG—Rate of mass change (differential thermogravimetry).

In the temperature range of 20–120 °C, a decrease in sample mass occurs, corresponding to the loss of hygroscopic moisture. In the range of 250–270 °C, the removal of hydrated moisture takes place, which proceeds smoothly without distinct peaks. As the temperature increases to 650–810 °C, the dehydration of magnesium hydrosilicates occurs. Some shifts in thermal effects may be associated with the presence of impurities, primarily iron oxides, as well as differences in the heating rate of the sample.

2.2. Carbothermic Reduction Roasting of Nickel Ore

According to the thermal analysis data on moisture removal and loss on ignition, this process positively influences the chemical composition of the ore by increasing the concentration of its components. However, it does not affect the nickel-to-iron ratio, meaning that the resulting alloy will contain 5.0–6.0% nickel. Therefore, the selective reduction of nickel and a controlled portion of iron become important considerations, as nickel has a higher reducibility than iron.

The technological flowchart for processing lateritic nickel ores and smelting nickel-containing ferroalloys using the metallothermic method is presented in Figure 3.
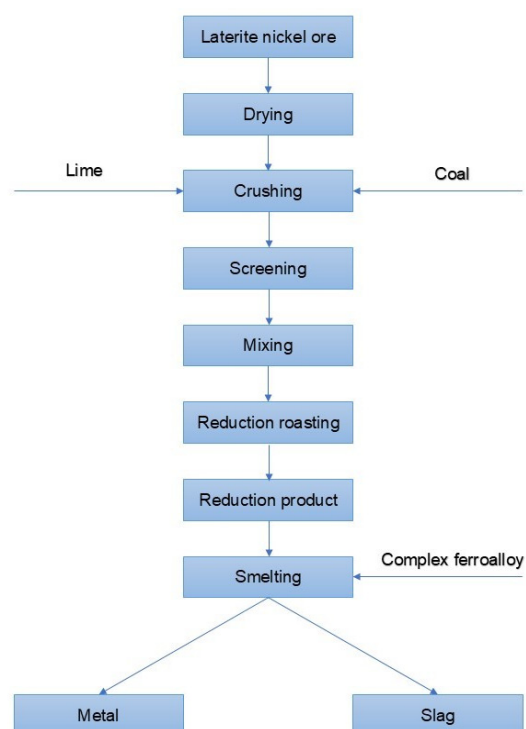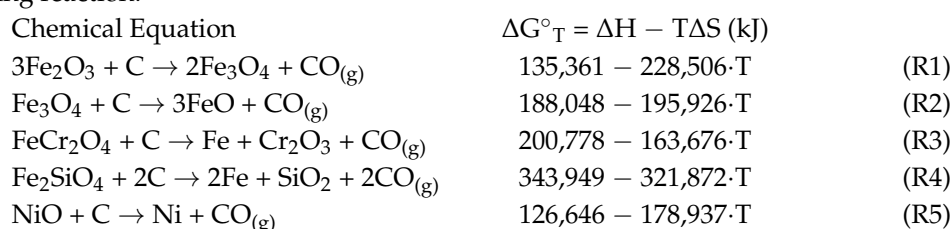
Figure 3. Technological flowchart of lateritic nickel ore processing and production of nickel-containing ferroalloy by the metallothermic method.

The procedure was carried out as follows: First, all charge materials were crushed and passed through a sieve with a diameter of 2.0 mm, as mentioned earlier. Second, the selection of the reductant and flux was performed. Coal was used as the reducing agent, with its chemical and technical composition presented in Table 2.

Table 2. Chemical and technical composition of coal, %.

C	A^c	V	W^p	S	Al_2O_3	SiO_2	MgO	CaO	Fe_2O_3	P_2O_5
51.55	5.7	31.45	10.95	0.35	25.21	59.71	2.6	4.24	7.8	0.44

The amount of reductant was determined based on the stoichiometric requirement for the complete reduction of higher iron oxides to lower oxides, as well as the decomposition of certain complex iron-based compounds into simpler substances according to the following reaction:

Chemical Equation	$\Delta G^{\circ}_T = \Delta H - T\Delta S$ (kJ)	
$3Fe_2O_3 + C \rightarrow 2Fe_3O_4 + CO_{(g)}$	$135{,}361 - 228{,}506 \cdot T$	(R1)
$Fe_3O_4 + C \rightarrow 3FeO + CO_{(g)}$	$188{,}048 - 195{,}926 \cdot T$	(R2)
$FeCr_2O_4 + C \rightarrow Fe + Cr_2O_3 + CO_{(g)}$	$200{,}778 - 163{,}676 \cdot T$	(R3)
$Fe_2SiO_4 + 2C \rightarrow 2Fe + SiO_2 + 2CO_{(g)}$	$343{,}949 - 321{,}872 \cdot T$	(R4)
$NiO + C \rightarrow Ni + CO_{(g)}$	$126{,}646 - 178{,}937 \cdot T$	(R5)

The calculation of Gibbs free energy change (ΔG, kJ) was performed using the "Chemistry 10" software package, Reaction Equation module, and the results showed that the reduction of hematite begins at T = 320 °C, the reduction of magnetite occurs at T = 690 °C, while for reactions (R3) and (R4), the reduction starts at T = 960 °C and T = 800 °C, respectively, and for the reduction of nickel (reaction (R5)), a relatively low temperature of T = 440 °C is required.

Thus, from a thermodynamic perspective, to reduce higher iron oxides to lower oxides and to decompose complex compounds into simple phases, the temperature conditions for roasting in laboratory conditions were set at T = 1150 °C. The reduction roasting time was selected as t = 90 min, with a holding time at T = 1150 °C of t = 30 min.

Lime (CaO > 93%) was used as the fluxing material. The lime addition was 20 g per 100 g of ore. It is necessary that during the smelting of nickel-containing ferroalloy by the metallothermic method, the final slag composition falls within the crystallization region of diopside (CaO·MgO·2SiO$_2$), which has a melting temperature of T = 1350–1370 °C. This requirement is explained by the CaO-MgO-SiO$_2$ phase diagram, which indicates that if the slag phase enters the monticellite region (CaO·MgO SiO$_2$) with a melting temperature of T = 1430 °C or the merwinite region (3CaO·MgO SiO$_2$) with a melting temperature of T = 1436 °C, it would lead to an increase in slag basicity (CaO/SiO$_2$ > 1.0) and a rise in the crucible smelting temperature.

After selecting the reducing agent and flux, the third step was the thorough mixing of the charge materials and their loading into an alumina crucible. The charge composition was calculated based on 100 g of nickel ore. The reduction roasting was carried out using a high-temperature furnace, LHT 08/17 BO (Nabertherm, Lilienthal, Germany), which allows experiments to be conducted in an oxidizing atmosphere with a programmable heating rate up to 1700 °C. The reduction roasting process of nickel ore with coal and CaO was carried out as follows: the furnace heating parameters were set using a pre-programmed sequence. First, the crucible (three alumina crucibles were used per experiment) with the charge materials was loaded into the furnace, and the heating program was activated. In the first 30 min, the furnace was heated to 300 °C. Then, as mentioned earlier, within 90 min, the temperature reached 1150 °C, followed by a 30-min holding period at this temperature. After roasting, the furnace with the samples was cooled to 50 °C. The crucibles were removed from the furnace, and the roasted product was weighed, with an average mass loss of 20% compared to the initial weight. Further, samples from the reduction roasting products were taken for chemical analysis and X-ray phase analysis.

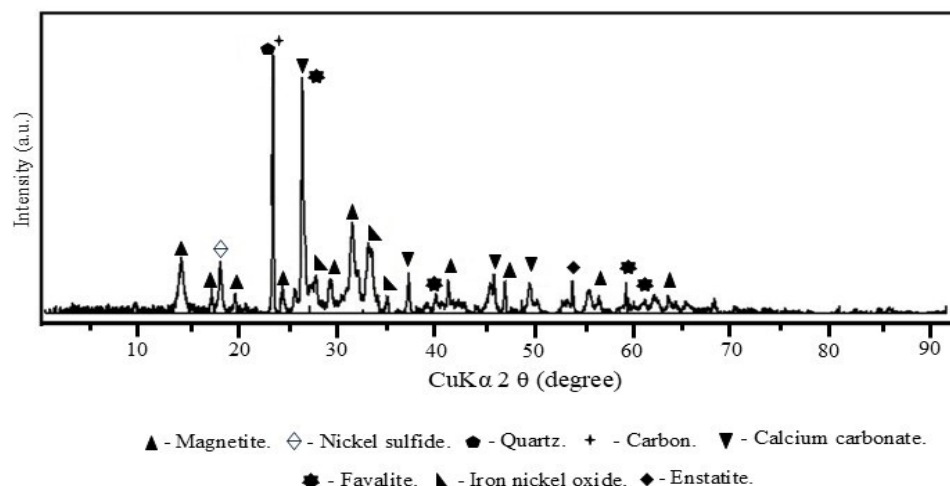### 2.3. Metallothermic Reduction of Nickel Ore

In order to obtain a nickel-containing alloy using the metallothermic method under laboratory conditions, we first conducted a thermodynamic modeling calculation for the simultaneous reduction of nickel, iron, and chromium using silicon and aluminum in a complex alloy within the temperature range of 500–1700 °C. The gas phase pressure was set at 1 atmosphere. The thermodynamic calculation was performed using the HSC Chemistry 10 software, specifically the "Equilibrium Compositions" module. This program enables the calculation of product quantities under isobaric and isothermal conditions after defining the quantitative, qualitative, and phase states of the initial substances [27–30].

The working system was based on SiO$_2$-CaO-Al$_2$O$_3$-NiO-FeO, which characterizes the composition of the product after reduction roasting. The amount of reducing agent was varied within the range of 5–35% of the total mass (100 g) of the reduction roasting product. The iron oxide to nickel oxide ratio in the working system was set at FeO/NiO = 25.

The modeling was conducted to determine the reduction degree of nickel (φ_{Ni}), iron (φ_{Fe}), and chromium (φ_{Cr}), depending on the amount of reductant added (5–35%) within the temperature range of 500–1700 °C. The reduction degree of the elements was calculated as the ratio of the mass in the metallic state (m_{Me}) to the initial mass ($m_{Me}^{initial}$).

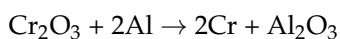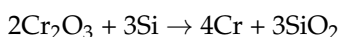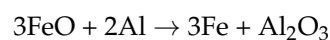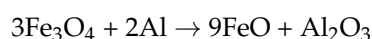$$\varphi_{Me} = \frac{m_{Me}}{m_{Me}^{initial}} \cdot 100 \qquad\qquad (R6)$$

The dependence of the extraction degree of nickel (φ_{Ni}), iron (φ_{Fe}), and chromium (φ_{Cr}) on the reducing agent consumption (5–35%) at temperatures T = 500 °C, T = 1000 °C, T = 1500 °C, and T = 1700 °C is presented in Figure 4.

▲ - Magnetite. ◇ - Nickel sulfide. ● - Quartz. + - Carbon. ▼ - Calcium carbonate.
● - Fayalite. ▲ - Iron nickel oxide. ◆ - Enstatite.

Figure 4. X-ray diffraction (XRD) pattern of the product after reduction roasting.

To verify the results of the thermodynamic modeling of the simultaneous reduction of nickel, iron, and chromium using silicon and aluminum as a complex reductant, we conducted laboratory experiments on the smelting of nickel-containing ferroalloy using the metallothermic method. As the initial material, we used the product after reduction roasting, whose chemical composition is presented in Table 3. The reducing agent used was a complex alloy with the following composition, %: Si—48%, Al—11%, Fe—30%, and P—0.01%. The calculation of the reductant was based on the following chemical reactions:

$$NiS + Si \rightarrow Ni + SiS$$

$$NiS + Al \rightarrow Ni + AlS$$

$$2Fe_3O_4 + Si \rightarrow 6FeO + SiO_2$$

$$2FeO + Si \rightarrow 2Fe + SiO_2$$

$$3Fe_3O_4 + 2Al \rightarrow 9FeO + Al_2O_3$$

$$3FeO + 2Al \rightarrow 3Fe + Al_2O_3$$

$$2Cr_2O_3 + 3Si \rightarrow 4Cr + 3SiO_2$$

$$Cr_2O_3 + 2Al \rightarrow 2Cr + Al_2O_3$$
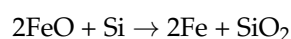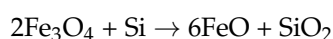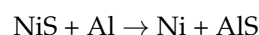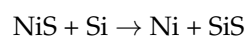
Table 3. Chemical composition of the product after reduction roasting, %.

Element	Fe$_{total}$	Ni$_{total}$	Cr$_2$O$_3$	SiO$_2$	CaO	Al$_2$O$_3$	C
Content (%)	60.5	2.60	2.80	38.40	21.70	2.80	2.20

The experiment was conducted with three variants of the charge weight. The reductant (a complex alloy) was added at 10%, 20%, and 30% of the amount of the product after the reduction roasting. The smelting of the nickel-containing ferroalloy was carried out using the same equipment that was used for the reduction roasting of nickel ore mixed with coal and CaO (LHT 08/17 BO "Nabertherm"). The crushed charge material (≤2.0 mm) was weighed and placed into alumina crucibles, which were then positioned in the furnace's

working zone at an initial temperature of 20 °C. The furnace temperature was gradually increased to 1600 °C. After the complete melting of the charge materials, a holding time of 15 min was maintained. Upon completion, the crucibles were removed from the furnace and cooled, and samples of metal and slag were collected for chemical analysis.

For the quantitative and qualitative analysis of the experimental alloy composition, an electron probe microanalyzer (EPMA) JXA-8230 (JEOL, Tokyo, Japan) was used. The analysis was performed at an accelerating voltage of 20 kV, an electron beam current of up to 5 nA, and a dead time of up to 20%, in combination with scanning electron microscopy (SEM) and energy-dispersive X-ray spectroscopy (EDS). The specified imaging and microanalysis conditions allow for reliable observation and recording of structural features ranging from sub-micron fractions to hundreds of microns at magnifications from X40 to X2000.

3. Results and Discussion

Table 3 and Figure 4 present the chemical composition of the reduction roasting product and its X-ray diffraction (XRD) pattern.

The results of the chemical analysis and X-ray diffraction (XRD) pattern of the product after thermal treatment indicate that complex compounds, such as serpentine ($Mg_3[Si_2O_5]OH_4$) and anorthite ($CaAlSi_2O_8$), decomposed into simpler compounds such as enstatite ($Mg_2Si_2O_6$) and calcium carbonate ($CaCO_3$). At the same time, higher iron oxides ($Fe_2O_3 \rightarrow Fe_3O_4 \rightarrow FeO$) were reduced to lower oxides. Nickel was partially reduced and was detected in the form of nickel sulfide (millerite). After roasting, nickel oxide was no longer present in the product. The concentration of chromium oxide remained unchanged, similar to its content in the initial ore. The presence of carbon in the product can be considered as an additional reducing agent for the production of nickel-containing ferroalloy.

Figure 5 presents the results of thermodynamic modeling of the reduction process for nickel (φNi), iron (φFe), and chromium (φCr), depending on the consumption of the complex alloy used as a reducing agent within the range of 5–35% at various temperatures.

As seen from the modeling results, with an increase in the reductant consumption, the reduction degree of nickel (φ_{Ni}), iron (φ_{Fe}), and chromium (φ_{Cr}) increases uniformly. However, with a 30% reductant consumption, the reduction degree of nickel φNi decreases by 9.73% compared to a 25% reductant consumption. This is likely due to the increased activity of silicon and aluminum (excess reductant) as their concentration in the alloy increases. The optimal temperature condition for nickel reduction is 1500 °C. As the temperature increases, the reduction degree of nickel decreases, which is attributed to nickel losses into the gas phase in the form of $NiO_{(g)}$.

Regarding iron and chromium, their maximum reduction degrees were $\varphi_{Fe} = 96.89\%$ and $\varphi_{Cr} = 87.44\%$, respectively, at a reductant consumption of 30% and a temperature of 1700 °C. We assume that iron and chromium contribute to more extensive reduction by silicon and aluminum, as the increased reductant consumption at high temperatures enhances their reduction efficiency.

Table 4 presents the results of laboratory experiments on the smelting of nickel-containing ferroalloy. The chemical composition of the smelting products was determined using the wet chemistry method.
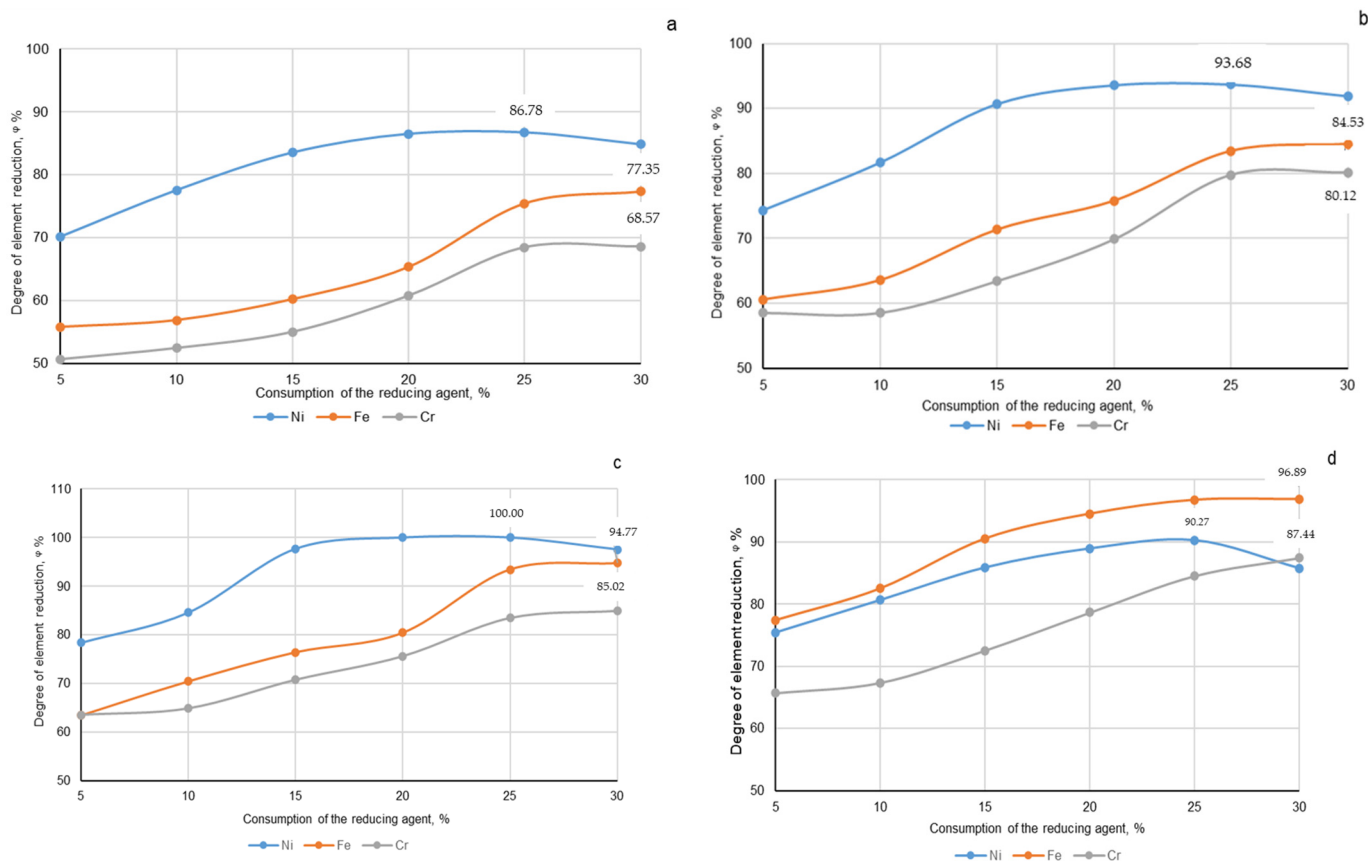
Figure 5. Dependence of the reduction degree of nickel, iron, and chromium elements on the reductant consumption based on the results of thermodynamic modeling: (**a**) t = 500 °C; (**b**) = 1000 °C; (**c**) = 1500 °C; (**d**) t = 1700 °C.

Table 4. Results of laboratory experiments on the smelting of nickel-containing ferroalloy.

| №	Products Obtained, g		Chemical Composition of the Metal, %				Chemical Composition of the Slag, %				
	Metal	Slag	Fe	Ni	Cr	Si	FeO	NiO	SiO_2	CaO	MgO
	Consumption of the reducing agent—10%										
1	15.3	52.2	80.8	10.2	3.2	4.3	9.7	0.8	52.4	30.2	5.8
2	17.2	61.4	82.6	9.7	2.8	3.3	8.6	1.2	53.2	28.4	6.8
3	16.4	58.3	80.7	11.3	4.3	3.1	8.3	1.1	52.1	27.4	4.9
	Consumption of the reducing agent—20%										
4	17.3	58.5	73.4	15.7	4.5	5.5	11.5	0.05	54.5	27.3	6.5
5	18.5	47.3	71.3	14.3	6.8	7.2	9.4	0.1	53.6	30.5	6.2
6	19.2	59.4	74.6	15.6	4.8	4.8	11.8	0.3	50.2	28.6	7.1
	Consumption of the reducing agent—30%										
7	16.8	58.4	75.7	6.5	2.7	13.3	12.6	0.5	57.4	28.4	-
8	18.8	55.6	74.5	7.3	2.8	14.5	13.2	0.4	55.4	25.6	-
9	19.3	57.4	72.8	6.6	3.1	17.4	13.2	0.6	59.5	21.7	1.3

Discussion of the laboratory experiment results:

- With a reducing agent consumption of 10%, the nickel concentration in the alloy did not exceed 10%. This is due to the insufficient amount of reducing agent, which causes

the nickel in the slag to remain as small metal particles. The low content of silicon and aluminum in the reducing agent reduces the rate of nickel settling, which, according to Stokes' law, does not allow it to fully transition into the metallic phase during the holding time. The element recovery was as follows: nickel—62.0%, iron—33.8%, and chromium—38.5%.

- With a 20% reducing agent consumption, better results were observed. In this case, an alloy with approximately 15% nickel content and 100% nickel recovery into metal was obtained, which is significantly higher than the results from the melts with lower reducing agent consumption. This result is explained by the fact that at a 20% reducing agent consumption, silicon and aluminum effectively reduce nickel. The iron content in the alloy decreased by 10% compared to the previous scenario, while iron recovery remained at 31.3%. Chromium recovery was 67.9%.

- With an increase in reducing agent consumption to 30%, the nickel concentration in the alloy decreased to 6.8%. However, the alloy became more enriched with silicon, with an average content of about 15%. This type of alloy has limited application in steel production but can be used as a reducing agent in ferro-nickel production due to its high silicon content. The element recoveries under these conditions were as follows: nickel—45.7%, iron—29.3%, and chromium—36.2%.

Figure 6 presents photographs of the fractured crucible with smelting products (a) and the nickel-containing alloy extracted from the crucible (b). In all laboratory experiments, the slag separated easily from the metal. Additionally, during the separation of slag from metal in smelting runs No. 1–3, metallic droplets were observed in the slag phase. As shown in Table 4, the slag-to-metal ratio was on average $m_{Slag}/m_{Me} = 3.2$.

(a)   (b)
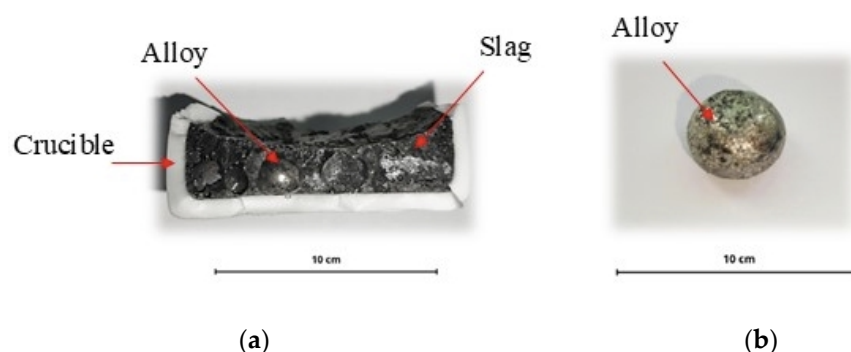
Figure 6. Images of the fractured crucible (**a**) and the nickel-containing alloy (**b**) after the experiment.

Figure 7a–k presents SEM images and EDS spectra of nickel-containing alloy particles. In Figure 7b (points A, C, D, E) and Figure 7g,i–k, particles of iron, nickel, chromium, and traces of calcium are observed, indicating that these elements were successfully reduced using the metallothermic method. Additionally, silicon and iron particles are specifically concentrated in Figure 7b (point B) and Figure 7h.

Using elemental mapping, it was determined that titanium appears in a finely dispersed form, while nickel exhibits larger, more extended structures. Point EDS microanalysis confirmed the overall structural-analytical pattern, showing that silicon (Si) dominates up to 14.89 wt. % and iron (Fe) reaches up to 76.38 wt. %. Nickel (Ni) is detected at concentrations up to 15.02 wt. %, and chromium (Cr) is present at up to 3.47 wt. %. It was also found that some particles exhibit a fine structure with gradual concentration variations, which is most clearly observed in linear EDS microanalysis. In these heterogeneous regions, the concentrations reached the following: nickel—up to 21.76 wt. %, chromium—up to 2.11 wt. %, and titanium—up to 1.01 wt. %; calcium was detected only in trace amounts. Additionally, chromium, nickel, and copper displayed co-phase behavior,

indicating a strong correlation in their distribution within the alloy. Table 5 presents the results of the quantitative analysis of the studied microscopic points of the experimental alloy using EPMA.
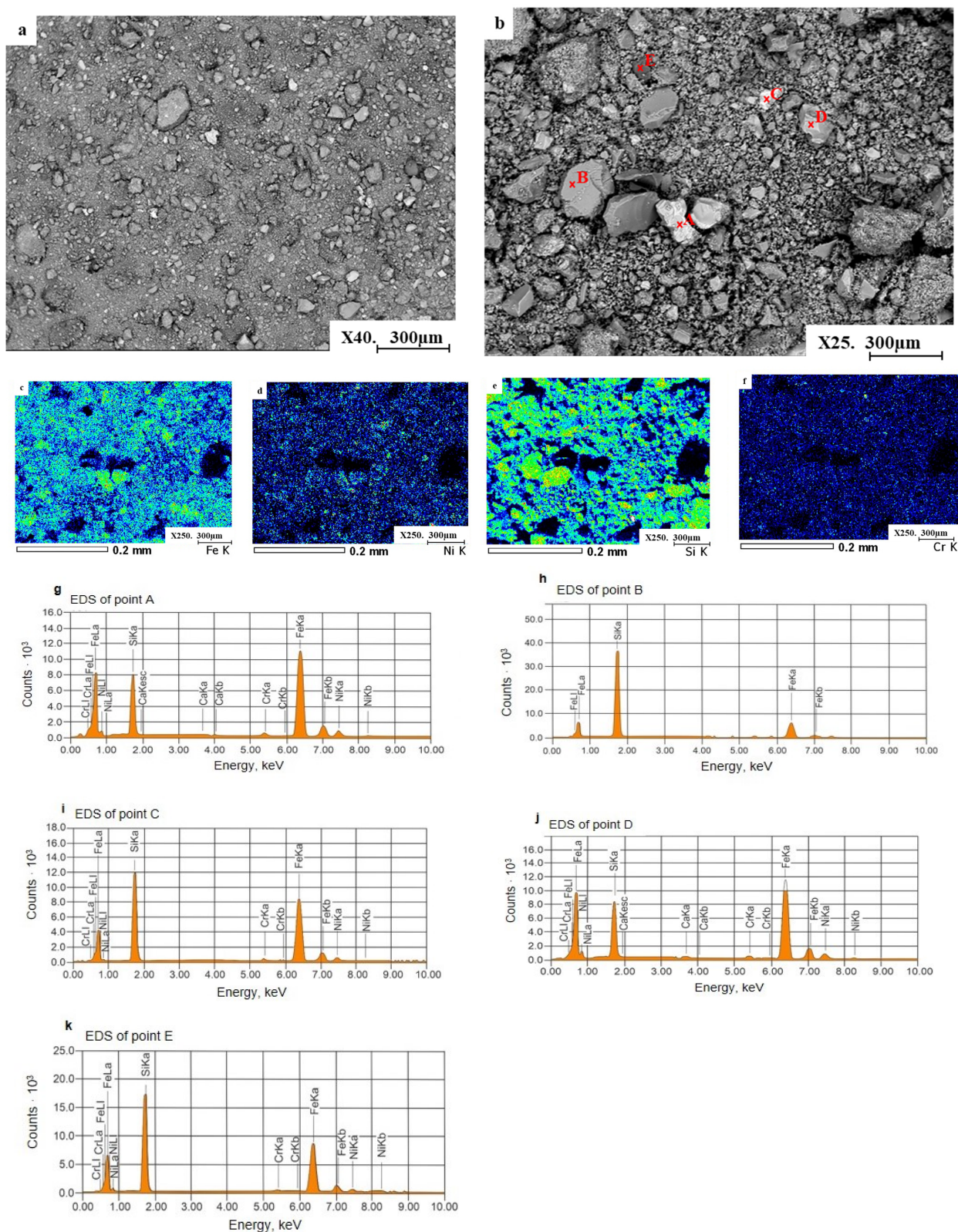
Figure 7. SEM images and EDS spectra of nickel-containing ferroalloy particles.

Table 5. Quantitative composition by microscopic points of the experimental alloy.

Element	Point A	Point B	Point C	Point D	Point E
Fe	75.84	45.11	70.15	76.38	63.11
Si	7.50	54.89	24.35	14.22	30.14
Ni	13.96	-	4.76	7.70	5.88
Cr	1.85	-	0.74	1.46	0.87
Total	100.00	100.00	100.00	100.00	100.00

4. Conclusions

Under laboratory conditions, a product was obtained for the subsequent production of nickel-containing ferroalloy. The results showed that under optimal process conditions—roasting temperature of 1150 °C, roasting time of 90 min, holding time at 1150 °C for 30 min, and CaO addition of 20 g—it was possible to obtain a product with the following composition: total Ni—2.60%, total Fe—60.5%, Cr_2O_3—2.80%, SiO_2—38.40%, and CaO—21.70%, with an Fe/Ni ratio of 25.

Through thermodynamic modeling, the reduction degree of nickel (φNi), iron (φFe), and chromium (φCr) was calculated depending on the amount of reductant added (5% to 35%) within the temperature range of 500–1700 °C. The calculation results showed that with an increase in reductant consumption, the reduction degree of nickel, iron, and chromium (φNi, φFe, φCr) increases uniformly. The maximum nickel reduction degree (φNi = 100%) was achieved at a reductant consumption of 25% at a temperature of 1500 °C. However, when the reductant consumption increased to 30%, the nickel reduction degree (φNi) decreased by 9.73%. Regarding iron and chromium, their maximum reduction degrees were φFe = 96.89% and φCr = 87.44%, respectively, at a reductant consumption of 30% and a temperature of 1700 °C. This phenomenon is explained by the fact that at higher temperatures and increased reductant consumption, iron and chromium undergo deeper reduction, leading to their higher recovery rates.

The fundamental feasibility of producing a nickel-containing alloy by the metallothermic method has been demonstrated using the product after reduction roasting and a complex alloy as the reducing agent, with the following chemical composition (%): Si—48, Al—11, Fe—30, and P—0.01, at a reductant consumption ranging from 10% to 30%. It was found that the optimal conditions for nickel reduction were achieved at a reductant consumption of 20%, resulting in an alloy containing 15% Ni and up to 5% Cr, with nickel and chromium extraction into metal reaching 100% and 67.9%, respectively. The obtained ferrochromium-nickel alloy can be used for the production of corrosion-resistant steel. Further increasing the reductant consumption to 30% led to an increase in silicon content in the alloy, reaching up to 15%, which makes the alloy suitable as a reductant for ferronickel production.

Thus, the study of lateritic nickel ore reduction conditions has demonstrated the feasibility of obtaining nickel-containing ferroalloy by the metallothermic method, using silicon and aluminum in a complex alloy as the reducing agents.

Data Availability Statement: The original contributions presented in this study are included in the article. Further inquiries can be directed to the corresponding authors.

Conflicts of Interest: Authors Gulnur Abikenova, Nurzhan Nurgali and Maral Almagambetov were employed by ERG Research and Engineering Center. The remaining authors declare that the research was conducted in the absence of any commercial or financial relationships that could be construed as a potential conflict of interest.

References

1. Extraction and Processing of Nickel-Cobalt Ores of the Kempirsai Group Deposits. Investment Proposals. Available online: https://invest.gov.kz/ru/doing-business-here/invest-projects/29980/ (accessed on 13 January 2025).
2. Kelamanov, B.; Yessengaliyev, D.; Sariev, O.; Akuov, A. Technological analysis of the production of nickel-containing composite materials. *J. Compos. Sci.* **2024**, *8*, 179. [CrossRef]
3. Processing of Cobalt-Nickel Ore. Investment Proposals. Available online: https://invest.gov.kz/ (accessed on 4 April 2025).
4. Farrokhpay, S.; Filippov, L.; Fornasiero, D. Pre-concentration of nickel in laterite ores using physical separation methods. *Miner. Eng.* **2019**, *141*, 105892. [CrossRef]
5. Li, J.H.; Li, Y.Y.; Zheng, S.; Xiong, D. Research review of laterite nickel ore metallurgy. *Nonferrous Met. Sci. Eng.* **2015**, *6*, 35–40.
6. Wang, Z.; Chu, M.; Liu, Z.; Wang, H.; Zhao, W.; Gao, L. Preparing ferro-nickel alloy from low-grade laterite nickel ore based on metallized reduction–magnetic separation. *Metals* **2017**, *7*, 313. [CrossRef]
7. Thorne, R.L.; Roberts, S.; Herrington, R. Climate Change and the Formation of Nickel Laterites. *Geology* **2012**, *40*, 331–334. [CrossRef]
8. Quast, K.; Connor, J.N.; Skinner, W.; Robinson, D.J.; Addai-Mensah, J. Preconcentration strategies in the processing of nickel laterite ores Part 1: Literature review. *Miner. Eng.* **2015**, *79*, 261–268. [CrossRef]
9. Yessengaliev, D.; Mukhametkhan, M.; Mukhametkhan, Y.; Zhabalova, G.; Kelamanov, B.; Kolesnikova, O.; Shyngysbayev, B.; Aikozova, L.; Kaskataeva, K.; Kuatbay, Y. Studies of the Possibility of Improving the Quality of Iron Ores and Processing of Technogenic Composite Iron-Containing Waste of Metallurgical Production. *J. Compos. Sci.* **2023**, *7*, 501. [CrossRef]
10. Sadykhov, G.B.O.; Kisilev, A.I.; Lainer, Y.A. Method for Processing Nickel Laterite Ores Resulting in the Direct of Ferronickel. WO2014133421, 4 September 2014.
11. Butt, C.; Cluzel, D. Nickel laterite ore deposits. *Weather. Serpentinites Elem.* **2013**, *9*, 123–128.
12. Brand, N.W.; Butt, C.R.M.; Elias, M. Nickel Laterites: Classification and Features. *AGSO J. Aust. Geol. Geophys.* **1998**, *17*, 81–88.
13. Gleeson, S.A.; Butt, C.R.M.; Elias, M. Nickel Laterites: A Review. *SEG Discov.* **2003**, *54*, 1–18. [CrossRef]
14. Lin, B. Rotary Kiln for Producing Ferronickel from Indonesia Sulawesi Nickel Laterite Ore Through RKEF (Rotary Kiln-Electric Furnace) Technical Processing. CN 202973836, 5 June 2013.
15. Keskinkilic, E. Nickel Laterite Smelting Processes and Some Examples of Recent Possible Modifications to the Conventional Route. *Metals* **2019**, *9*, 974. [CrossRef]
16. Lv, X.; Wang, L.; You, Z.; Dang, J.; Lv, X.; Qiu, G.; Bai, C. Preparation of Ferronickel from Nickel Laterite Ore via Semi-molten Reduction Followed by Magnetic Separation. In *Extraction 2018*; Springer: Cham, Switzerland, 2018; pp. 913–920. [CrossRef]
17. Yildirim, H.; Morcali, H.; Turan, A.; Yucel, O. Nickel pig iron production from laterite nickel ores. In Proceedings of the Thirteenth International Ferroalloys Congress: Efficient Technologies in Ferroalloy Industry, Almaty, Kazakhstan, 9–13 June 2013.
18. McIntyre, T.V. The Riddle Nickel Enterprise—A Study in Resource Geography. Master's Thesis, Oregon State University, Oregon, OR, USA, 1962.
19. Zayakin, O.V. Development of a Rational Composition and Technology for the Production of Nickel-Containing Ferroalloys from Low-Grade Oxidized Nickel Ores. Ph.D. Thesis, Institute of Metallurgy, Ural Branch of the Russian Academy of Sciences, Yekaterinburg, Russia, 2002.
20. Schodde, R.; Guj, P. Nickel: A tale of two cities. *Geosyst. Geoenviron.* **2025**, *4*, 100356. [CrossRef]
21. Nurjaman, F.; Adhalia, D.; Sari, Y.; Astuti, W.; Sumardi, S.; Haryono, T.; Nulhakim, L.; Petrus, H.T.B.M.; Saptoro, A.; Prasetya, A. Valorization of Solid Residue from the Lateritic Nickel Ore Leaching Process for Ferronickel Production. *Waste Biomass Valorization* **2025**, *16*, 1511–1520. [CrossRef]
22. Zhang, W.; Ma, B.; Wang, C.; Chen, Y. Study on the treatment of pyrolysis products from the nitric acid pressure leach liquor of laterite. *Sep. Purif. Technol.* **2024**, *350*, 127780. [CrossRef]
23. Yessengaliyev, D.; Kelamanov, B.; Sariev, O.; Kuanalin, Y. Research of thermal analysis of nickel ore and mixture with carbon-containing reducing agents by non-isothermal method. *Metalurgija* **2024**, *63*, 344–346.

24. Murakami, H.; Miyazaki, K.; Honnami, K.; Okano, S.; Mochizuki, M. Parameter Optimization of Thermal Shrinkage Technique for Simple Numerical Simulation of Welding Angular Distortion. *ISIJ Int.* **2021**, *7*, 2143–2149. [CrossRef]

25. Rong, Y.; Xu, J. Forming Mechanism of Weld Cross Section and Validating Thermal Analysis Results Based on the Maximal Temperature Field for Laser Welding. *Metals* **2022**, *12*, 774. [CrossRef]

26. Djurdjevic, M.B. Application of thermal analysis in ferrous and nonferrous foundries. *Metall. Mater. Eng.* **2021**, *27*, 457–471. [CrossRef]

27. Roine, A. HSC Chemistry®, [Software] Metso: Outotec, Pori. 2021. Available online: www.mogroup.com/hsc (accessed on 1 February 2024).

28. Shevko, V.; Makhanbetova, B.; Aitkulov, D.; Badikova, A.; Amanov, D. Thermodynamic and Experimental Substantiation of Comprehensive Processing of Zinc Sulfide Ore and Its Concentration Tailings to Extract Non-Ferrous Metals and Produce a Silicon Ferroalloy. *Minerals* **2024**, *14*, 819. [CrossRef]

29. Yessengaliyev, D.; Kelamanov, B.; Zayakin, O. Thermodynamic modeling of the recovery process of manganese by metallothermic method. *J. Chem. Technol. Metall.* **2022**, *57*, 1230–1234.

30. Makhambetov, E.N.; Vorobkalo, N.R.; Baisanov, A.S.; Mynzhasar, E.A. Smelting of vanadium-containing alloys with using non-standard reducing agents. *CIS Iron Steel Rev.* **2023**, *25*, 21–25. [CrossRef]